

Electron Temperature and Density Measurements by Harmonic Electron Cyclotron Emissions from Doublet-III Tokamak Plasma

T. Yamamoto, M. Abe,^(a) T. Hirayama, A. Kameari,^(b) A. Kitsunezaki, K. Kodama, S. Konoshima, M. Nagami, S. Sengoku, M. Shimada, N. Suzuki, T. Takizuka, and M. Washizu^(c)

Japan Atomic Energy Research Institute, Tokai, Naka, Ibaraki, Japan

(Received 7 August 1984)

The intensity ratio of the second- to the third-harmonic cyclotron emission, measured by a scanning Fourier-transform spectrometer, is investigated for a wide range of discharge parameters. Dependences of the ratio on electron temperature and density are described by the model of plane parallel walls. The time evolution of central electron density deduced from the ratio is consistent with multichannel CO₂ interferometer data within the estimated experimental error.

PACS numbers: 52.40.Db, 52.70.Gw

Measurement of electron cyclotron emission (ECE) from a tokamak plasma is one of the most useful diagnostic methods to obtain local information on the electron temperature T_e and density n_e . In particular, optically thick harmonics of ECE have been successfully employed to deduce the electron temperature.¹⁻⁵ The technique of electron density measurement from the emission of optically thin harmonics, however, has not been established as yet.^{3,6-8} This is because the signal-to-noise ratio of these harmonic signals is not high enough and reflection on the vacuum vessel wall obscures the localization of the emission. Recently, an optically thin emission of the third harmonic for $f_{pe}/f_{ce} \geq 1$ (f_{pe} is the electron plasma frequency and f_{ce} the electron cyclotron frequency) has been investigated experimentally in the Heliotron-E.⁹ In this Letter we present the first successful results of local electron density measurement by means of the second- and third-harmonic emissions from a tokamak plasma. The emission for the extraordinary mode is measured for a wide range of plasma parameters, $0.6 \leq f_{pe}/f_{ce} \leq 1.3$ and $0.7 < T_e < 4.0$ keV, where the effect of energetic electrons is relatively small.¹⁰ For the present plasma, the optical depth for second-harmonic emission is more than 3 and that for third-harmonic emission is in the range of 0.02-3.

In order to obtain local information more accurately, the intensity ratio of the second- to the third-harmonic emission is investigated. The specific intensity ratio $R_{23} = I_2/I_3$ of the second and third harmonics of ECE is given in the plane-parallel-walls model by

$$I_n = n^2(1 - e^{-\tau_n}) / (1 - \rho e^{-\tau_n}), \quad (1)$$

where ρ is the effective reflectivity of the vacuum vessel wall. The optical depth τ_n for the extraordinary mode is given by¹¹

$$\tau_n = \frac{\pi^2 n^2 (n-1)}{2^{(n-1)} (n-1)!} Z_n(x) \left(\frac{kT_e}{m_0 c^2} \right)^{n-1} \frac{f_{ce}}{c} R, \quad (2)$$

with

$$Z_n(x) = x \left(\frac{1 - (x/n^2)(n^2 - x)}{n^2 - x - 1} \right)^{n-3/2} \left(1 + \frac{x/n}{n^2 - x - 1} \right)^2,$$

where $x = (f_{pe}/f_{ce})^2$, m_0 is the electron rest mass, c the light velocity, and R the major radius. Local information on the ratio is available in the absence of overlapping of the neighboring harmonics. The no-overlap region of the third harmonic is $\frac{3}{2}(R_0 - a) > R > \frac{3}{4}(R_0 + a)$, where R_0 is R of the magnetic axis and a is the plasma minor radius.

The experiment is carried out in the Doublet-III tokamak, which has a doublet-shaped vacuum vessel with major radius 1.43 m, minimum width at the vessel midplane 0.8 m, maximum width at the center of the D-shaped plasma 1.04 m, and height 3.0 m. For the present experiments, noncircular plasmas with $a \approx 0.4$ m are produced in the upper half of the vacuum vessel with or without additional neutral-beam-injection heating. Discharge parameters are as follows: toroidal magnetic field $B_t = 2.1-2.4$ T, plasma current $I_p = 500-700$ kA, and $n_e = (2-8) \times 10^{19} \text{ m}^{-3}$. The experimental setup and the characteristics of the discharge are described by Nagami *et al.*¹²

The far-infrared Michelson interferometer developed by Costley *et al.*¹³ is used as the electron cyclotron spectrometer. The setup of the interferometer and the data processing of the frequency spectrum from an interferogram were reported in detail in Ref. 10. The frequency resolution is about 10 GHz, which corresponds to about 10-cm spatial resolution along the major radius at $B_t = 2.4$ T. The interferometer is capable of producing a complete interferogram in less than 15 msec. The line of sight of the spectrometer is the same horizontal plane as that for the Thomson scattering measurement. The laser beam of the Thomson scattering system passes vertically at $R = 1.48$ m through the plasma.

The intensity ratio at $R = 1.48$ m obtained by ECE measurement is shown in Figs. 1(a) and 1(b) as functions of the temperature and the density measured by the Thomson-scattering system, respectively. The curves in Fig. 1(a) show the calculated results from Eq. (1) with an effective reflectivity ρ of 0.0 to 0.6 at $n_e = 5 \times 10^{19} \text{ m}^{-3}$. The solid curves in Fig. 1(b) show the calculated results for $\rho = 0.2$ and the broken curves those for $\rho = 0.4$ for $T_e = 1.75\text{--}2.25$ keV. By comparison of the calculated results with the measured ones in both Figs. 1(a) and (b), the effective reflectivity of $\rho = 0.2 \pm 0.1$ is chosen as the best approximation. This low reflectivity is reasonably explained by the facts that the Doublet-III tokamak has the big vacant space at the bottom half of the vacuum vessel and the wall surface is rough because of arrays of backup limiters and partially consists of armor tiles made of TiC-coated carbon.

Although it is easy to calculate R_{23} if T_e and n_e are given, the inversion process to obtain T_e from R_{23} and n_e or n_e from R_{23} and T_e is difficult. For this purpose a numerical code is developed, based on iteration by the Newton-Raphson technique. The n th harmonic emission is peaked at a frequency given by

$$f_n = n f_{ce}(R) \left[1 - \left(n + \frac{1}{2} \right) k T_e / m_0 c^2 \right]$$

for fixed R .¹⁴ $T_e(R)$ can be computed from the measured intensity ratio $I_2(f_2)/I_3(f_3)$ by an iteration process until a self-consistent result is obtained. The calculation is valid for $x < 1.8$ in which Z_2 and Z_3 are single valued. Comparison between the temperature derived from the ECE measurement with use of the code and the one from the Thomson-scattering system for a wide range of plasma parameters is shown in Fig. 2. The horizontal bars show the error of the Thomson-scattering system.

We now consider the error in the temperature calculated by the method mentioned above. From Eqs. (1) and (2), the relative variation in the temperature due to a small change in the values of R_{23} and n_e is given in the incremental approximation by

$$\frac{\delta T_e}{T_e} = \frac{1}{2} \left[\frac{1}{K} \left(\frac{\delta R_{23}}{R_{23}} + L \frac{\delta \rho}{\rho} \right) + J \frac{\delta n_e}{n_e} \right], \quad (3)$$

with $K = |(\tau_3/R_{23})\partial R_{23}/\partial \tau_3|$, $L = |(\rho/R_{23})\partial R_{23}/\partial \rho|$, and $J = |(x/Z_3)\partial Z_3/\partial x|$. In the present experiments, $\tau_2 > 3$ and I_2 is almost constant as seen in Eq. (1). It should be noted that the value of L for $\tau_3 \ll 1$ becomes very large as ρ approaches unity and the black-body emission of the third harmonic leads to the divergence of the estimated error through $K = 0$. The systematic errors δR_{23} arising from the measurement technique are a calibration error of the frequency response and a spatial resolution error. The spatial resolution error is estimated to be small near the plas-

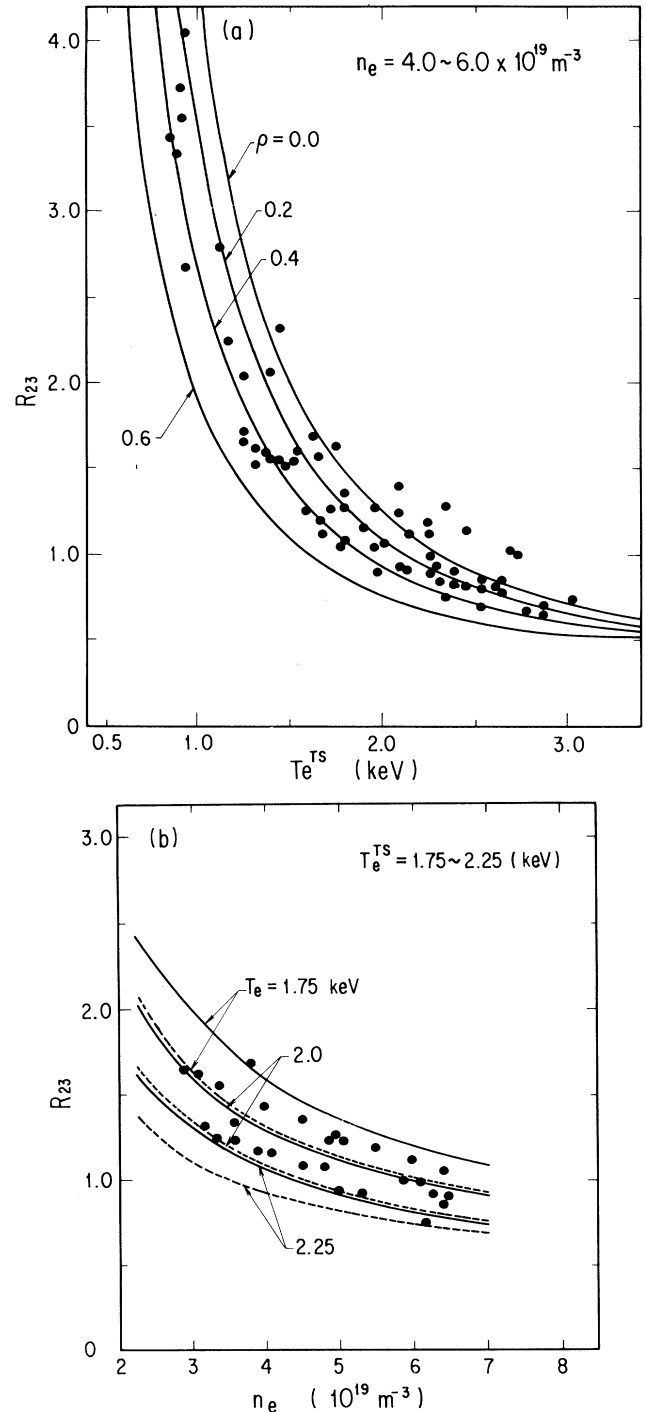


FIG. 1. (a) Intensity ratio of the second to third harmonic, R_{23} , at the major radius $R = 1.48$ m vs electron temperature. The temperature and the density are obtained from Thomson scattering. The curves show the calculated results with the effective reflectivity ρ of the vacuum vessel wall at $n_e = 5.0 \times 10^{19} \text{ m}^{-3}$ as a parameter. (b) Intensity ratio vs electron density. The solid and broken curves show the calculated ones at $\rho = 0.2$ and 0.4 , respectively, as a parameter of the electron temperature.

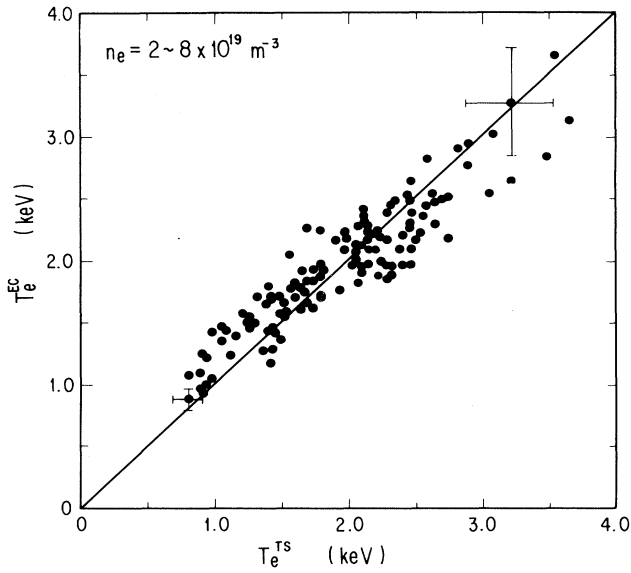


FIG. 2. Electron temperature T_e^{EC} calculated with the measured R_{23} and the Thomson-scattering density n_e vs the Thomson-scattering temperature T_e^{TS} .

ma center over most of the profiles,⁷ and hence the uncertainty in the measurement of the ratio is less than 0.05.⁸ Taking $\delta R_{23}/R_{23} = 0.05$, $\delta\rho/\rho = 0.5$ obtained above, and $\delta n_e/n_e$ from the error of the Thomson-scattering density measurement, we calculate the error of the temperature measurement from Eq. (3) and the typical errors are shown in Fig. 2 as the vertical bar. Most of the data points show good agreement between the two temperatures within the experimental errors.

We can also compare the local electron density derived from the ECE measurement with that measured by other diagnostic methods. Figures 3(a) and 3(b) show the time evolution of the line-integrated densities measured by three horizontal CO₂ laser interferometers and the density derived from the ECE measurement at $R = 1.48$ m. The temperature, which is used in the density calculation, is obtained from the second-harmonic emission and is shown in Fig. 3(c). The intensity of the second-harmonic emission is calibrated by the Thomson scattering for several shots. The error bar of the density, as shown in Fig. 3(b), is calculated from Eq. (3) with $\delta T_e/T_e = 0.05$. As shown in the figure, the density derived from ECE agrees well with the CO₂ laser interferometer data within the estimated error during the discharge. The plasma is produced by the limiter discharge with $I_p = 520$ kA and neutral-beam injection of ≈ 6 MW. The density drop near the plasma center during the high-power neutral-beam injection is clearly detected

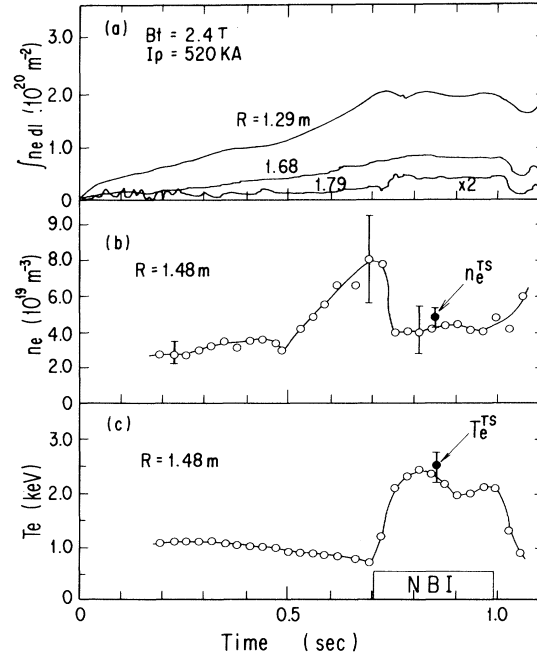


FIG. 3. (a) Line-integrated electron densities in the equatorial plane measured by three-channel horizontal CO₂ laser interferometers for three radial positions. R is the minimum major radius of the CO₂ beam chord. (b) Time evolution of the local electron density at $R = 1.48$ m computed from the measured R_{23} and the electron temperature obtained from the calibrated second-harmonic emission, as shown in (c). For the same shot and radial position, the density and the temperature obtained at $t = 880$ msec with the Thomson-scattering system are also shown in (b) and (c), respectively.

by the ECE measurement.

In summary, it has been shown that the intensity ratio of the second- to the third-harmonic emission is in good agreement with calculated results using the plane-parallel-walls model having a low effective reflectivity of the vacuum vessel wall. This makes it possible to obtain the electron temperature from ECE measurement without an absolute intensity calibration of the radiometer if density is known and the reflectivity is less than ~ 0.1 . The low reflectivity may be made by placing a radiation dump in the vacuum vessel opposite to a receiving antenna of high angular resolution. Moreover, this method is useful to obtain the time behavior of the local electron density in the absence of overlapping of the harmonics.

The authors are very grateful to Dr. S. Mori, Dr. Y. Iso, Dr. Y. Obata, Dr. K. Tomabechi, Dr. M. Yoshikawa, Dr. M. Tanaka, Dr. T. Iijima, and Dr. Y. Tanaka at Japan Atomic Energy Research Institute and Dr. T. Ohkawa and Dr. J. R. Gilleland at GA Technologies for their continuous support of our work. In particular, the authors wish to thank Dr. F. P. Blau and

Dr. E. Fairbanks for the fine adjustment of the far-infrared Michelson interferometer. It is our pleasure to acknowledge the fine support of the Doublet-III diagnostics group under Dr. R. Fisher and Dr. J. Baur, the neutral-beam-injection group under Dr. A. Colleraine, and the machine operation group under Dr. R. Callis. This work was performed under a cooperative agreement between the Japan Atomic Energy Research Institute and the United States Department of Energy under Department of Energy Contract No. DE-AT03-80SF11512.

^(a)On leave of absence from Hitachi Ltd.

^(b)On leave of absence from Mitsubishi Atomic Power Industries, Inc.

^(c)On leave of absence from Toshiba Corp.

¹TFR Group, in *Proceedings of the Seventh European Conference on Controlled Fusion and Plasma Physics, Lausanne, Switzerland, 1975* (European Physical Society, Geneva, 1975), Vol. 1, 14B.

²J. Hosea, V. Arunasalam, and R. Cano, *Phys. Rev. Lett.*

39, 408 (1977).

³F. J. Stauffer and D. A. Boyd, *Infrared Phys.* **18**, 755 (1978).

⁴R. Cano, A. A. Bagdasarov, A. B. Berlizov, E. P. Gorbunov, and G. E. Notkin, *Nucl. Fusion* **19**, 1415 (1979).

⁵G. E. Tait, F. J. Stauffer, and D. A. Boyd, *Phys. Fluids* **24**, 719 (1981).

⁶D. A. Boyd, *Int. J. Infrared Millimeter Waves* **1**, 45 (1980).

⁷W. H. M. Clark, *Plasma Phys.* **25**, 1501 (1983).

⁸F. P. Blau, in *Proceedings of the Sixth International Conference on Infrared and Millimeter Waves*, Miami Beach, Florida, December 1981 (unpublished).

⁹J. N. Talmadge, H. Zushi, S. Sudo, T. Mutoh, M. Sato, T. Obiki, O. Motojima, A. Iiyoshi, and K. Uo, *Phys. Rev. Lett.* **52**, 33 (1984).

¹⁰A. C. Riviere, F. P. Blau, R. P. Chase, E. S. Fairbanks, and T. W. Petrie, General Atomic Company, San Diego, Report No. GA-A 16605, 1981 (unpublished).

¹¹M. Bornatici, *Plasma Phys.* **24**, 629 (1982).

¹²M. Nagami *et al.*, *Nucl. Fusion* **24**, 183 (1984).

¹³A. E. Costley, R. J. Hastie, J. W. M. Paul, and J. Chamberlain, *Phys. Rev. Lett.* **33**, 758 (1974).

¹⁴C. M. Celata and D. A. Boyd, *Nucl. Fusion* **17**, 735 (1977).